RC24069 (W0610-023) October 4, 2006
Materials Science

IBM Research Report

Low Dielectric Constant Nanocomposite Thin Films Based on Silica Nanoparticle and Organic Thermosets

Qinghuang Lin, Stephan A. Cohen, Lynne Gignac, Brian Herbst, David Klaus, Eva Simonyi, Jeffrey Hedrick, John Warlaumont
IBM Research Division
Thomas J. Watson Research Center
P.O. Box 218
Yorktown Heights, NY 10598

Hae-Jeong Lee, Wen-li Wu
Polymer Division
National Institute of Standards and Technology
Gaithersburg, MD 20899

Research Division
Almaden - Austin - Beijing - Haifa - India - T. J. Watson - Tokyo - Zurich

LIMITED DISTRIBUTION NOTICE: This report has been submitted for publication outside of IBM and will probably be copyrighted if accepted for publication. It has been issued as a Research Report for early dissemination of its contents. In view of the transfer of copyright to the outside publisher, its distribution outside of IBM prior to publication should be limited to peer communications and specific requests. After outside publication, requests should be filled only by reprints or legally obtained copies of the article (e.g., payment of royalties). Copies may be requested from IBM T. J. Watson Research Center , P. O. Box 218, Yorktown Heights, NY 10598 USA (email: reports@us.ibm.com). Some reports are available on the internet at http://domino.watson.ibm.com/library/CyberDig.nsf/home .

Low Dielectric Constant Nanocomposite Thin Films Based on Silica Nanoparticle and Organic Thermosets[#]

Qinghuang Lin*, Stephen A. Cohen, Lynne Gignac, Brian Herbst, David Klaus, Eva Simonyi, Jeffrey Hedrick, John Warlaumont

IBM T.J. Watson Research Center, P.O. Box 218, Yorktown Heights, New York 10598

Hae-Jeong Lee and Wen-li Wu

Polymer Division, National Institute of Standards and Technology, Gaithersburg, MD 20899

Abstract

Low dielectric constant (low-*k*) nanocomposite thin films have been prepared by spin coating and thermal cure of solution mixtures of one of two organic low-*k* thermoset pre-polymers and a silica nanoparticle with an average diameter of about 8 nm. The electrical, the mechanical, and the thermo-mechanical properties of these low-*k* nanocomposite thin films have been characterized with 4-point probe electrical measurements,

---

[#] Official contribution of the National Institute of Standards and Technology, not subject to copyright in the United States.

To whom all correspondence should be addressed: Phone: 914-945-2366, Fax: 914-945-2141, Email: qhlin@us.ibm.com

nanoindentation measurements with an atomic force microscope (AFM), and specular X-ray reflectivity. Addition of the silica nanoparticle to the low-*k* organic thermosets enhances both the modulus and the hardness and reduces the coefficient of thermal expansion of the resultant nanocomposite thin films. The enhancements in the modulus of the nanocomposite thin films are less than those predicted by the Halpin-Tsai equations, presumably due to the relatively poor interfacial adhesion and/or the aggregation of the hydrophilic silica nanoparticles in the hydrophobic organic thermoset matrices. The addition of the silica nanoparticle to the low-*k* organic thermoset matrices increases the relative dielectric constant of the resultant nanocomposite thin films. The relative dielectric constant of the nanocomposite thin films has been found to agree fairly well with an additive formula based on the Debye equation.

Key Words: low dielectric constant nanocomposite; thin film; mechanical property; electrical property; structure-property relationship.

Introduction

The relentless drive to ever smaller semiconductor devices has necessitated, among other things, novel on-chip electrical insulators to improve signal speed and quality as well as to reduce power consumption. These electrical insulators, called low permittivity or low dielectric constant (low-*k*) materials with *k* less than that of silicon oxide ($k = 4.3$), can be organic or inorganic materials[1,2]. They can be prepared by either the "wet" spin coating[3,4] or the "dry" plasma enhanced chemical vapor deposition (PECVD)[5,6] methods.

One such low-*k* material is a class of organic thermosets with *k* less than 3.0. A prominent example of these novel electronics materials is an organic low-*k* material, called SiLK with a $k = 2.65$[3]. SiLK, which is produced by and a trade mark of the Dow Chemical Company[*], is a highly crosslinked polyphenylene. It is derived from a cyclopentadienone monomer and a multifunctional acetylene-containing monomer. Its synthesis involves the 4+2 cycloaddition reaction of the cyclopentadienone and the multifunctional acetylene-containing monomers to form a soluble polyphenylene pre-polymer. This cycloaddition is followed by the expulsion of CO to form a crosslinked polyphenylene during curing. The multifunctional nature of the SiLK monomers leads to a crosslinked polyphenylene thermoset after a full thermal cure[3]. The chemical structures of the SiLK organic low-*k* pre-polymer and the cured thermoset are shown in Scheme 1.

Given the organic nature of the SiLK low-*k* material, it possesses some remarkable properties including the combination of a low dielectric constant ($k = 2.65$), high thermal stability up to 425 ^{o}C, excellent toughness and good adhesion to substrates when an adhesion promoter is used[3,7]. It has been shown by IBM to afford excellent structural integrity, performance improvement as well as electrical reliability for the 90 nm node generation of devices[8]. Unfortunately, the relatively weak mechanical properties of SiLK and its poor mismatch of coefficient of thermal expansion (CTE) with copper wires and substrates have prevented a wide adoption of SiLK in high-volume semiconductor manufacturing.

---

[*] Certain commercial equipment and materials are identified in this paper in order to specify adequately the experimental procedure. In no case does such identification imply recommendation by the National Institute of Standards and Technology nor does it imply that the material or equipment identified is necessarily the best available for this purpose.

Table 1 lists key properties of silicon oxide and the SiLK low-*k* material. The SiLK low-*k* material has a significantly lower dielectric constant than that of silicon oxide. Its modulus and hardness, however, are more than an order of magnitude lower than those of silicon oxide. Moreover, the CTE of SiLK can be more than two orders of magnitude higher than that of silicon oxide. This higher CTE of SiLK causes a serious mismatch in its CTE with copper wires and silicon substrates. These relatively weak mechanical properties and the CTE mismatch of the SiLK low-*k* material pose significant challenges to the fabrication and the reliability of advanced computer chips with a SiLK/copper interconnect. Although the weak mechanical properties may be circumvented with clever chip designs, the CTE mismatch is particularly troublesome as it leads to unacceptable failures during the deep thermal cycling reliability tests. Clearly, improvements in the mechanical and the thermo-mechanical properties of SiLK are desirable if it is to be widely adopted in high-volume semiconductor manufacturing.

The objectives of this work are to enhance the mechanical properties and to reduce the CTE of SiLK with a nanocomposite approach. The nanocomposite concept has attracted increasing attention in the last decade or so due to the demonstrated and the potential improvements to the physical properties and the performance of polymeric materials[9-28]. These improvements to the physical properties include enhanced modulus, fracture toughness, increased heat distortion temperature, reduced CTE and flammability, as well as enhanced processability[9,13,16,18,19,29-36]. Previous work on nanocomposites has been focused mostly on engineering polymeric materials. Very little nanocomposite work has

been published on electronics materials in order to improve their mechanical and thermo-mechanical properties although nanometer-scale sacrificial organic pore generators, called porogens, have been used extensively to generate nanoporous low-*k* materials[6,37-43].

In this paper, we present our work on nanocomposite thin films of two SiLK low-*k* materials and a silica nanoparticle with an average diameter of about 8 nm. We prepared the nanocomposite thin films by spin coating and thermal cure of solution mixtures of one of the SiLK low-*k* thermoset pre-polymers and the silica nanoparticle. We characterized the electrical, the mechanical and the thermo-mechanical properties of the nanocomposite thin films with 4-point probe electrical measurements, nanoindentation measurements, and specular X-ray reflectivity. We also characterized the morphology of the silica / SiLK nanocomposite thin films with a high-resolution transmission electron microscope (TEM). The structure-property relationship of these nanocomposite thin films will be discussed.

Experimental

Materials

The organic thermoset low-*k* materials used in this study are SiLK-D and SiLK-I. Both SiLK-D and SiLK-I resins are based on the same crosslinked polyphenylene material platform. SiLK-D resin, however, has lower CTE values than those of SiLK-I, particularly at elevated temperatures. For instance, The CTE values of SiLK-I can be as

high as 160 ppm/^{o}C, whereas those of SiLK-D are below 100 ppm/^{o}C within a temperature range from room temperature to 450 ^{o}C. These two SiLK low-*k* materials were obtained in pre-polymer solutions from the Dow Chemical Company.

The silica nanoparticle, IPA-ST-S, was obtained from Nissan Chemicals as a 20 % by weight isopropanol solution. This as-received nanoparticle was not an electronics-grade material as it had high metallic impurities (Table 2). The as-received silica nanoparticle solution was concentrated from 20 % by weight to 30 % or 40 % by weight of silica content by evaporating part of the isopropanol solvent. The average diameter of the silica nanoparticles was reported by the supplier to be about 8 nm.

Two types of 200 mm silicon wafers were used in this work: a lightly boron-doped type with a resistivity of 9 to18 Ω for nanoindentation and X-ray reflectivity measurements and a heavily boron-doped type with a resistivity of 0.005 to 0.01 Ω for electrical measurements. The lightly boron-doped wafers were used as received. The heavily boron-doped wafers underwent a 4-step cleaning process to remove the backside silicon oxide and contaminants prior to spin-coating. First, the wafers were dipped in a dilute HF solution and then went through a 40:1:1 by volume mixture of water, hydrogen peroxide, and ammonium hydroxide at 35 ^{o}C and then a 100:1 by volume mixture of water and hydrochloric acid at about 60 ^{o}C. Lastly the wafers were rinsed with high-purity water and dried.

Film Preparation

Nanocomposite solutions were prepared by mixing a SiLK pre-polymer solution and the concentrated silica nanoparticle solution to form homogeneous solutions. The highest concentrations of the silica nanoparticle in the nanocomposite films were 25 % and 40 % by weight, respectively, for the nanocomposite films containing SiLK-D and SiLK-I. The volume concentrations of the silica nanoparticle were calculated by using densities of 2.1 g/cm^3 and 1.1 g/cm^3 for the silica nanoparticle and the SiLK resin, respectively.

Nanocomposite thin films were prepared by spin coating of the nanocomposite solutions on 200 mm silicon wafers with a Brewer Science spin coater at a spin speed of 2000 rpm to 3000 rpm. The as-coated films were baked at 200 ^oC to remove solvent and further cured at 450 ^oC for 2 h under a N_2 atmosphere in a horizontal furnace.

Characterization

Thickness Measurements

Film thickness was measured with a KLA-Tencor P-10 profilometer. Each thickness was the average of 6 measurements. The film thickness was about 500 nm for films used for electrical measurements and more than 1000 nm for films used for nanoindentation measurements, respectively. The 1000 nm films were prepared by double coating of the nanocomposite formulations with an intervening bake at 200 ^oC. These thicker films were used for the nanoindentation measurements in order to minimize the substrate effect.

Electrical Measurements

The relative dielectric constant (*k*) measurements of the low-*k* nanocomposite thin films were performed in an enclosed Electroglas 2001X wafer prober with a high isolation Temptronic hot chuck in concert with an HP4275A LCR meter. Metal-on-semiconductor structures were tested at 100 *K*Hz under an inert N_2 atmosphere and a Keithley 230 voltage source was used to provide DC bias to ensure full charge (majority carriers) accumulation in the substrate. Al dots of various sizes (500 nm in thickness) were deposited on top of the low-*k* nanocomposite thin films and a blanket Al film of 500 nm in thickness was deposited on the backside of the highly boron-doped silicon wafers prior to electrical measurements. Coaxial probes were used to contact the 1.27 mm diameter Al dots and back contact was achieved through the wafer chuck.

Measurements were carried out at both 23 ^{o}C and 150 ^{o}C. For the 150 ^{o}C measurements, the samples were heated from room temperature to 150 ^{o}C with a ramp rate of about 15 ^{o}C/min by the hot chuck and held at 150 ^{o}C for 15 min in a N_2 atmosphere prior to the measurements. Each dielectric constant number was the average of 3 measurements. Each breakdown curve was the results of 56 measurements of leakage current density versus electrical field for each sample.

Nanoindentation

Modulus and hardness data were acquired using a nanoindentation method. Nanoindentation was performed with a Nano Intender XP system (Nano Instruments Innovation Center), equipped with the Dynamic Contact Module (DCM). The DCM

provides an overall miniaturization of the XP system, making it more suitable to perform indentations in low force ranges (0.01 mN to 12 mN). The DCM machine used a Berkovitch indenter (angle 65.3°). The Continuous Stiffness Measurement (CSM) option was used[44]. This technique superimposes a small oscillatory force to the indentation force to allow continuous measurements of modulus and hardness during the indentation process. Tip calibration was based on the Oliver-Pharr method[44]. A stiffness change of 4 times was used as an indicator to detect the surface. A constant strain rate was maintained during each indentation test. The modulus or the hardness values were taken at the lowest point of the modulus or the hardness versus indentation depth curves. The thickness of the nanocomposite films for the nanoindentation tests was more than 1000 nm to minimize the substrate effect. Each modulus or hardness value was the average of 20 indents.

Specular X-Ray Reflectivity

For integration of a low-*k* dielectric material, the coefficient of thermal expansion (CTE) of the low-*k* material is a key factor in successful fabrication and subsequent reliability tests. In this work, specular x-ray reflectivity (SXR) was utilized to monitor the changes in film thickness with an Å resolution as a function of temperature from 25 °C to 175 °C under a vacuum of approximately 1.33×10^{-3} Pa.

SXR measurements were performed using a modified high-resolution x-ray diffractometer in a θ–2θ configuration at the specular conditions, where the incident angle was equal to the detector angle, utilizing finely focused Cu K_{α} radiation with a

wavelength, λ, of 1.54 Å. The incident and the reflected beams were conditioned with a four-bounce germanium (220) monochromator and a three-bounce germanium (220) channel cut crystal, respectively. The reflected intensity was collected as a function of the grazing incident angle over an angular range of 0.1° to 1.0° with an angular reproducibility of ± 0.0001°. Initially the samples were annealed at 175 °C for 1 h under vacuum to outgas and to remove potential contaminants. SXR measurements were then performed at 25 °C, 75 °C, 125 °C, and 175 °C, incrementally with 1 h allowed between temperatures for thermal equilibration.

TEM

The morphology of the silica / SiLK nanocomposite was examined with a combination of focused ion beam (FIB) and high-resolution transmission electron microscopy (TEM) using a single beam 200 TEM FIB and a JEOL 4000 TEM microscope. The TEM samples were prepared by the FIB sectioning and an *ex-situ* lift-out method. Details of this method can be found in the literature[45,46].

Results and Discussion

Nanocomposites of Silica / Organic Low-k Thermosets

The SiLK organic low-*k* material is a highly crosslinked polyphenylene. It possesses some remarkable properties including the combination of a low dielectric constant (k = 2.65), high thermal stability up to 425 °C, and excellent toughness [3,7]. However, its

relatively weak modulus and hardness, coupled with its CTE mismatch with copper wires and silicon substrates, pose significant challenges to the fabrication and the reliability of advanced computer chips with a SiLK / copper interconnect.

We have adopted a nanocomposite approach to improving the mechanical and the thermo-mechanical properties of the SiLK low-*k* material. Our objectives are to enhance the modulus and the hardness and to reduce CTE of the SiLK low-*k* material with a nano-filler. The nano-filler of nanocomposites for on-chip insulator application has to meet many stringent criteria, including superior mechanical properties (modulus, hardness, etc.), a significantly lower CTE than that of the SiLK organic matrix, a low dielectric constant and good electrical properties, a small particle size (< 10 % of minimum critical dimension), good dispersion in and adhesion with the SiLK organic matrix.

In this study, a silica nanoparticle (with an average diameter of about 8nm) was selected as the nano-filler. This silica nanoparticle has a hydrophilic surface which is rich in silanol groups [47]. The silica / SiLK nanocomposite thin films were prepared by spin coating, followed by thermal cure of solution mixtures of the silica nanoparticle and a SiLK pre-polymer. Two versions of the SiLK organic low-*k* materials were used in this study, SiLK-I and SiLK-D. Both have a dielectric constant of about 2.65. SiLK-D has smaller CTE values than those of SiLK-I, particularly at elevated temperatures.

The silica nanoparticle and the SiLK organic low-*k* materials formed crack-free nanocomposite thin films when the silica nanoparticle concentration was less than 27.5 %

by volume. When the silica nanoparticle concentration exceeded 27.5 % by volume, instantaneous cracking of the nanocomposite films was observed after thermal cure even though homogeneous solution mixtures of the two nanocomposite components and crack-free as-coated films were obtained.

Morphology of Silica / Organic Thermoset Nanocomposites

The morphology of the silica / organic thermoset nanocomposite thin films was investigated with a high-resolution transmission electron microscope. The morphology of these nanocomposite thin films exhibits a nearly uniform global distribution of the silica nanoparticles or nanoparticle aggregates (Figure 1a). However, distinct local aggregation of the silica nanoparticles was also observed (Figure 1b). The sizes of these local aggregates range from the apparent single silica nanoparticle to several hundreds of nanometers which would contain thousands of individual nanoparticles. This local aggregation is not entirely unexpected given the hydrophilic nature of the silica nanoparticle surface and the hydrophobic nature of the organic thermoset matrix.

As discussed previously, the SiLK organic low-*k* materials are made of highly aromatic hydrocarbon compounds. Like many other hydrocarbon materials, they have a distinct hydrophobic nature. They exhibit a very low moisture adsorption as evidenced by the nearly identical relative dielectric constant (k) values at room temperature and an elevated temperature of 150 ^{o}C for the neat SiLK-I and SiLK-D resins (see discussion later). The silica nanoparticle is known to undergo hydrolysis to form a layer of silanol on its

surface[47]. It is, therefore, not unexpected that the silica nanoparticles would form local aggregates in the nanocomposite thin films.

It has been reported that surface modification of silica nanoparticles was effective to enhance dispersion and to improve adhesion of the silica nanoparticles in an organic matrix [48,49]. It is expected that a similar approach for the current silica / organic thermoset nanocomposite systems could lead to similarly desirable effects.

Effect of Silica Nanoparticle on Modulus and Hardness

Addition of the silica nanoparticle enhances the modulus and the hardness of the SiLK organic low-*k* thermosets. The improvements in the mechanical properties, however, are not as dramatic as those reported in the literature[9,13,16,18,19,31,36,50], where an order of magnitude of improvement was not uncommon. Figure 2 shows the improvements in the elastic modulus of both versions of the SiLK organic low-*k* thermosets. A similar effect of the silica nanoparticle on the hardness of the SiLK organic low-*k* thermosets has also been observed (Figure 3). The modulus and the hardness data are rather scattered even with a large number (20) of measurements for each data point. This is attributed to the non-uniform morphology of the silica / organic thermoset nanocomposite thin films where local aggregates of various sizes of the silica nanoparticles have been observed.

The improvements in the elastic modulus of SiLK-I and SiLK-D are about 50 % and 47 % for nanocomposites containing 27.5 % and 16.0 % by volume of the silica nanoparticle,

respectively. The improvements in the hardness of SiLK-I and SiLK-D are about 42 % and 29 % for nanocomposites containing 27.5 % and 16.0 % by volume of the silica nanoparticle, respectively. These improvements are not as significant as those reported in the literature[31,36,50]. As shown earlier, the primary reason for these poorer improvements in modulus and hardness appears to be the poor dispersion of the hydrophilic silica nanoparticles in the hydrophobic SiLK matrix. It is also speculated that poor interfacial bonding between the silica nanoparticle and the SiLK matrices may also contribute to these poorer improvements in the mechanical properties of the silica / SiLK low-*k* nanocomposite thin films.

The elastic modulus of a composite material can be described by the Halpin-Tsai equations

$$\frac{E}{E_m} = \frac{1+\xi\eta V_f}{1-\eta V_f} \qquad (1)$$

where

$$\eta = \frac{(E_f / E_m) - 1}{(E_f / E_m) + \xi} \qquad (2)$$

Where E is the modulus of the composite;

E_f is the modulus of the filler;

E_m is the modulus of the matrix;

V_f is the volume fraction of the filler.

ξ is a measure of filler reinforcement of the composite and is dependent on filler geometry, packing geometry, and loading conditions. In this work, we use a value of 2 for ξ in the Halpin-Tsai equations for the spherical nanoparticle filler.

Comparison of the measured modulus values and those calculated with the Halpin-Tsai equations are shown in Figures 2. In general, the measured modulus values are lower than those predicted by the Halpin-Tsai equations in both the SiLK-I and the SiLK-D nanocomposites. As is well-known, the Halpin-Tsai equations can be reduced to the rules of mixtures when $\xi = \infty$. The discrepancy between the experimental modulus values and those predicted by Halpin-Tsai equations in this work is in contrast to some of the observations of clay-based nanocomposites in the literature; In these clay-based nanocomposite systems, a general good agreement between the experimental values and the rules of mixtures was observed[9,31]. In super-hard inorganic nanocomposites, hardness was found to even exceed those predicted by the rules of mixtures[50].

Effect of Silica Nanoparticle on Coefficient of Thermal Expansion

Addition of the silica nanoparticle has a detectable influence on the coefficient of thermal expansion (CTE) of the resultant nanocomposite thin films. In this work, specular x-ray reflectivity (SXR) was utilized to monitor the changes in silica / SiLK nanocomposite

film thickness with an Å resolution as a function of temperature from 25 °C to 175 °C under a vacuum of approximately 1.33×10^{-3} Pa. The thickness of the nanocomposite thin films varied nearly linearly with temperature (Figure 4). The CTE values were calculated by a linear curve fitting of the thickness data at various temperatures. The CTE values thus obtained were the out-of-the-plane values.

The out-of-the-plane CTE of SiLK-I was determined to be $(121 \pm 5) \times 10^{-6}$ ppm/^{o}C[+] in a temperature range from room temperature to 175 ^{o}C. For the nanocomposite containing 12.5 % by volume of the silica nanoparticle, this out-of-the-plane CTE value was reduced to $(90 \pm 6) \times 10^{-6}$ /^{o}C in the same temperature range. This represents a 25.6 % reduction in the out-of-the-plane CTE and brings the CTE of the resultant nanocomposite low-*k* film closer to that of the copper wires.

In summary, addition of the silica nanoparticle to the SiLK low-*k* materials does enhance the modulus and the hardness as well as reduce the CTE of the neat SiLK resins. This nanocomposite approach could be a material alternative to help alleviating the reliability failures of a neat SiLK/copper interconnect during the deep thermal cycling reliability tests.

[+] The data throughout the manuscript and in the figures are presented along with the standard uncertainty (±) involved in the measurement.

Effect of Silica Nanoparticle on Dielectric Constant

The variation of the relative dielectric constant of the silica / organic thermoset nanocomposite thin films exhibits two salient features (Figures 5a and 5b); First, the dielectric constant values of the silica / organic thermoset nanocomposite thin films show varied dependence on the silica nanoparticle content, depending on the amount of the silica nanoparticle in the nanocomposites. For both sets of the nanocomposite thin films, the dielectric constant of the nanocomposite thin films increases slightly for nanocomposites containing less than 10 % by volume of the silica nanoparticle. In contrast, it increases rapidly with the silica nanoparticle content when the silica nanoparticle content exceeds 10 % by volume.

Second, as in many other low-*k* materials, the dielectric constant of the nanocomposite thin films was observed to have higher values at 23 ^{o}C than those at 150 ^{o}C with an identical silica nanoparticle concentration. This phenomenon is generally attributed to the desorption of moisture from the low-*k* materials prior to and during the high temperature electrical measurements at 150 ^{o}C. Moisture (H_2O) has a much higher relative dielectric constant than those of the SiLK low-*k* resins and silicon oxide. The evaporation of moisture from the nanocomposite thin films at 150 ^{o}C thus decreases the dielectric constant measured at the elevated temperature.

The relative dielectric constant (*k*) of a dielectric material is a macroscopic property of the material. It is related to its microscopic parameters through the Debye equation as follows[1]:

$$\frac{k-1}{k+2}=\frac{N}{3k_0}(\alpha_e+\alpha_d+\frac{\mu^2}{3KT}) \quad \text{…………………(3)}$$

Where k is the relative dielectric constant of a dielectric material to that of vacuum;

k_0 is the dielectric constant of vacuum;

N is number of molecules per unit volume;

α_e is the electronic polarization;

α_d is the distortion polarization;

μ is the orientation polarizability;

K is the Boltzmann constant;

T is temperature.

Assuming molar additivity of the polarizability, for a two-component nanocomposite, it then follows:

$$\frac{k-1}{k+2}=V_f\frac{k_f-1}{k_f+2}+(1-V_f)\frac{k_m-1}{k_m+2} \quad \text{……………..(4)}$$

Where k, k_f, k_m are the relative dielectric constants of the composite, the filler, and the matrix, respectively;

V_f is the volume fraction of the filler.

The relative dielectric constant of the silica / organic thermoset nanocomposites can thus be calculated with known relative dielectric constant values of the filler and the matrix as well as the volume fraction of the filler. In the present work, the relative dielectric constant of the silica nanoparticle was chosen to be 4.3. The experimentally measured values of the relative dielectric constants of the organic thermoset matrices, SiLK-I and SiLK-D, were used in the calculations. To minimize possible complication of the contribution of the adsorpted moisture, comparison of the calculated relative dielectric constant values are made with the experimental ones only at 150 ^{o}C.

The predicted *k* values of the silica / organic thermoset nanocomposite thin films agree fairly well with the experimental ones. Figures 5a and 5b also show the comparison of the measured and the calculated relative dielectric constant values of the nanocomposite thin films based on SiLK-I and SiLK-D. The calculated relative dielectric constant values are in good agreement with the experimental ones without any fitting parameter. The experimental *k* values are generally slightly higher than the calculated values. This is presumably due to the residual moisture and/or the hydroxyl group (-OH) on the surfaces of the silica nanoparticles, both of which have higher relative dielectric constants than that of pure silicon dioxide (k = 4.3).

Effect of Silica Nanoparticle on Dielectric Breakdown and Leakage Current Density

Addition of the silica nanoparticle has an adverse effect on the dielectric breakdown and the leakage current density of the resultant nanocomposite thin films. Both the dielectric

breakdown voltage and the leakage current density deteriorate with increasing amount of the silica nanoparticle in the nanocomposites. Figures 6 and 7 show the electrical current density *vs*. field (J-V) curves and the breakdown voltage of the silica / SiLK-I nanocomposite thin films. Similar results were obtained for the silica / SiLK-D nanocomposite thin films (not shown). In this work, the dielectric breakdown voltage or field is defined as the onset electrical field at which the leakage current density starts to rise sharply till breakdown in the J-V curves. The leakage current density is taken as the current density at 2 MV/cm electrical field of the J-V curves.

The leakage current density and the breakdown voltage of the neat SiLK-I resin are $< 1X10^{-9}$ A/cm^2 and 5 MV/cm, respectively. These are quite respectable values for an organic low-*k* material. This leakage current density, however, increases steadily with increasing amount of the silica nanoparticle concentration in the nanocomposites (Figure 6).

Addition of the silica nanoparticle also has a deleterious effect on the breakdown voltage of the resultant nanocomposite thin films. The breakdown voltage decreases continuously with increasing amount of the silica nanoparticle in the nanocomposites (Figure 7). This deleterious effect of the silica nanoparticle on the leakage current density and the breakdown voltage is attributed to the excessive impurity in the silica nanoparticle solution used in this study. The impurity contents of the as-received silica nanoparticle solution are listed in Table 2. The values of some key contaminants range from tens of part per billion (ppb) to about 0.5 %. Most of these contaminants have

concentrations several orders of magnitude larger than those required of electronic-grade low-*k* materials, which are generally less than a few to tens of ppb. Clearly, a significant improvement in the purity of the silica nanoparticle solution is needed if it were to be used in low-*k* materials.

Summary and Conclusions

Low dielectric constant (low-*k*) nanocomposite thin films have been prepared by spin coating and thermal cure of solution mixtures of one of two organic low-*k* thermoset pre-polymers and a silica nanoparticle with an average diameter of about 8 nm. Addition of the silica nanoparticle to the low-*k* organic thermosets enhances both the modulus and the hardness and reduces the coefficient of thermal expansion of the resultant nanocomposite thin films. The lower modulus values of the nanocomposite thin films, as compared with those predicted by the Halpin-Tsai equations, are ascribed to the relatively poor interfacial adhesion and/or the aggregation of the hydrophilic silica nanoparticles in the hydrophobic organic thermoset matrices. The addition of the silica nanoparticle to the low-*k* organic thermoset matrices increases the relative dielectric constant of the resultant nanocomposite thin films. The relative dielectric constant of the nanocomposite thin films has been found to agree fairly well with the additive formula based on the Debye equation.

Acknowledgement

The authors would like to thank Prof. Raymond Pearson for suggesting the Halpin-Tsai equations for the nanocomposite thin films reported in this paper.

References

1 Maex, K.; Baklanov, M. R.; Shamiryan, D.; Iacopi, F.; Brongersma, S. H.; Yanovitskaya, Z. S. Journal of Applied Physics 2003, 93, 8793.

2 Morgen, M.; Ryan, E. T.; Zhao, J.-H.; Hu, C.; Cho, T. H.; Ho, P. S. Annual Review of Materials Science 2000, 30, 645.

3 Martin, S. J.; Godschalx, J. P.; Mills, M. E.; Shaffer, E. O.; Townsend, P. H. Advanced Materials 2000, 12, 1769.

4 Miller, R. D.; Volksen, W.; Lee, V. Y.; Connor, E.; Matgbitang, T.; Zafran, R.; Sundberg, L.; Hawker, C. J.; Hedrick, J. L.; Huang, E.; Toney, M.; Huang, Q. R.; Frank, C. W.; Kim, H. C. In Polymers for Microelectronics and Nanoelectronics; Lin, Q.; Pearson, R. A.; Hedrick, J. C., Eds.; American Chemical Society: Washington, DC, 2004, p 144.

5 Grill, A.; Patel, V. Journal of Applied Physics 1999, 85, 3314.

6 Grill, A.; Patel, V. Applied Physics Letters 2001, 79, 803.

7 Tyberg, C.; Huang, E.; Hedrick, J.; Simonyi, E.; Gates, S.; Cohen, S.; Malone, K.; Wickland, H.; Sankarapandian, M.; Toney, M.; Kim, H.-C.; Miller, R.; Volksen, W.; Lurio, L. In Polymers for Microelectronics and Nanoelectronics; Lin, Q.; Pearson, R. A.; Hedrick, J. C., Eds.; American Chemical Society: Washington, DC, 2004, p 107.

8 Goldblatt, R. D.; Agarwala, B.; Anand, M. B.; Barth, E. B.; Biery, G. A.; Chen, Z. G.; Cohen, S.; Connolly, J. B.; Cowley, A.; Dalton, T.; Das, S. K.; Davis, C. R.; Deutsch, A.; DeWan, C.; Edelstein, D. C.; Emmi, P. A.; Faltermeir, C. G.; Jitzgimmons, J. A.; Hedrick, J. C.; Heidenreich, J. E.; Hu, C. K.; Hummel, J. P.; Jones, P.; Kaltalioglu, E.; Kastenmeier, B. E.; Krishnan, M.; Landers, W. F.; Linger, E.; Liu, J.; Lustig, N. E.; Malhotra, S.; Manger, D. K.; McGahay, V.; Mih, R.; Nye, H. A.; Purushothaman, S.; Rathore, H. A.; Seo, S. C.; Shaw, T. M.; Simon, A. H.; Spooner, T. A.; Stetter, M.; Wachnik, R. A.; Ryan, J. G. Proceedings of the International Interconnect Technology Conference, San Francisco, CA, 2000, pp 261.

9 Kojima, Y.; Usuki, A.; Kawasumi, M.; Okada, A.; Fukushima, Y.; Kurauchi, T.; Kamigaito, O. Journal of Materials Research 1993, 8, 1185.

10 Kojima, Y.; Usuki, A.; Kawasumi, M.; Okada, A.; Kurauchi, T.; Kamigaito, O. Journal of Polymer Science Part A-Polymer Chemistry 1993, 31, 1755.

11 Kojima, Y.; Usuki, A.; Kawasumi, M.; Okada, A.; Kurauchi, T.; Kamigaito, O. Journal of Polymer Science Part A-Polymer Chemistry 1993, 31, 983.

12 Komarneni, S. Journal of Materials Chemistry 1992, 2, 1219.

13 Usuki, A.; Hasegawa, N.; Kato, M. In Inorganic Polymeric Nanocomposites and Membranes, 2005, p 135.

14 Usuki, A.; Kato, M.; Okada, A.; Kurauchi, T. Journal of Applied Polymer Science 1997, 63, 137.

15 Usuki, A.; Kawasumi, M.; Kojima, Y.; Okada, A.; Kurauchi, T.; Kamigaito, O. Journal of Materials Research 1993, 8, 1174.

16 Usuki, A.; Koiwai, A.; Kojima, Y.; Kawasumi, M.; Okada, A.; Kurauchi, T.; Kamigaito, O. Journal of Applied Polymer Science 1995, 55, 119.

17 Usuki, A.; Kojima, Y.; Kawasumi, M.; Okada, A.; Fukushima, Y.; Kurauchi, T.; Kamigaito, O. Journal of Materials Research 1993, 8, 1179.

18 Giannelis, E. In Materials Chemistry, 1995, p 259.

19 Giannelis, E. P. Advanced Materials 1996, 8, 29.

20 Giannelis, E. P.; Krishnamoorti, R.; Manias, E. In Polymers in Confined Environments, 1999, p 107.

21 Balazs, A. C.; Singh, C.; Zhulina, E.; Lyatskaya, Y. Accounts of Chemical Research 1999, 32, 651.

22 Bourgeat-Lami, E.; Lang, J. Journal of Colloid and Interface Science 1998, 197, 293.

23 Cho, J. W.; Paul, D. R. Polymer 2001, 42, 1083.

24 Choi, J.; Harcup, J.; Yee, A. F.; Zhu, Q.; Laine, R. M. Journal of The American Chemical Society 2001, 123, 11420.

25 Gomez-Romero, P. Advanced Materials 2001, 13, 163.

26 Lu, Y. F.; Yang, Y.; Sellinger, A.; Lu, M. C.; Huang, J. M.; Fan, H. Y.; Haddad, R.; Lopez, G.; Burns, A. R.; Sasaki, D. Y.; Shelnutt, J.; Brinker, C. J. Nature 2001, 410, 913.

27 Messersmith, P. B.; Stupp, S. I. Journal of Materials Research 1992, 7, 2599.

28 Vaia, R. A.; Giannelis, E. P. MRS Bulletin 2001, 26, 394.

29 Agag, T.; Koga, T.; Takeichi, T. Polymer 2001, 42, 3399.

30 Chen, J. S.; Poliks, M. D.; Ober, C. K.; Zhang, Y. M.; Wiesner, U.; Giannelis, E. Polymer 2002, 43, 4895.

31 Fornes, T. D.; Paul, D. R. Polymer 2003, 44, 4993.

32 Garces, J. M.; Moll, D. J.; Bicerano, J.; Fibiger, R.; McLeod, D. G. Advanced Materials 2000, 12, 1835.

33 Hyun, Y. H.; Lim, S. T.; Choi, H. J.; Jhon, M. S. Macromolecules 2001, 34, 8084.

34 Kawasumi, M.; Hasegawa, N.; Kato, M.; Usuki, A.; Okada, A. Macromolecules 1997, 30, 6333.

35 Tyan, H. L.; Liu, Y. C.; Wei, K. H. Chemistry of Materials 1999, 11, 1942.

36 Zerda, A. S.; Lesser, A. J. Journal of Polymer Science Part B-Polymer Physics 2001, 39, 1137.

37 Brinker, C. J. MRS Bulletin 2004, 29, 631.

38 Grill, A.; Neumayer, D. A. Journal of Applied Physics 2003, 94, 6697.

39 Jeong, K. H.; Park, S. G.; Rhee, S. W. Journal of Vacuum Science & Technology B 2004, 22, 2799.

40 Lee, Y. J.; Huang, J. M.; Kuo, S. W.; Chang, F. C. Polymer 2005, 46, 10056.

41 Ramesh, S.; Shutzberg, B. A.; Huang, C.; Gao, J.; Giannelis, E. P. IEEE Transactions on Advanced Packaging 2003, 26, 17.

42 Venugopal, V. C.; Lakhtakia, A.; Messier, R.; Kucera, J. P. Journal of Vacuum Science & Technology B 2000, 18, 32.

43 Yang, S.; Mirau, P.; Sun, J.; Gidley, D. W. Radiation Physics and Chemistry 2003, 68, 351.

44 Liniger, E. G.; Simonyi, E. E. Journal of Applied Physics 2004, 96, 3482.

45 Giannuzzi, L. A.; Drown, J. L.; Brown, S. R.; Irwin, R. B.; Stevie, F. A. MRS Proc 1997, 480, 19.

46 Overwijk, M. H. F.; Vandenheuvel, F. C.; Bullelieuwma, C. W. T. Journal of Vacuum Science & Technology B 1993, 11, 2021.

47 Iler, R. K. The Chemistry of Silica: Solubility, Polymerization, Colloid and Surface Properties, and Biochemistry; Wiley: New York, 1979.

48 von Werne, T.; Patten, T. E. Journal of the American Chemical Society 1999, 121, 7409.

49 Sondi, I.; Fedynyshyn, T. H.; Sinta, R.; Matijevic, E. Langmuir 2000, 16, 9031.

50 Veprek, S.; Argon, A. S. Journal of Vacuum Science & Technology B 2002, 20, 650.

Figures and Tables

Scheme 1: Chemical structures of the SiLK low-*k* materials[3] used in this study

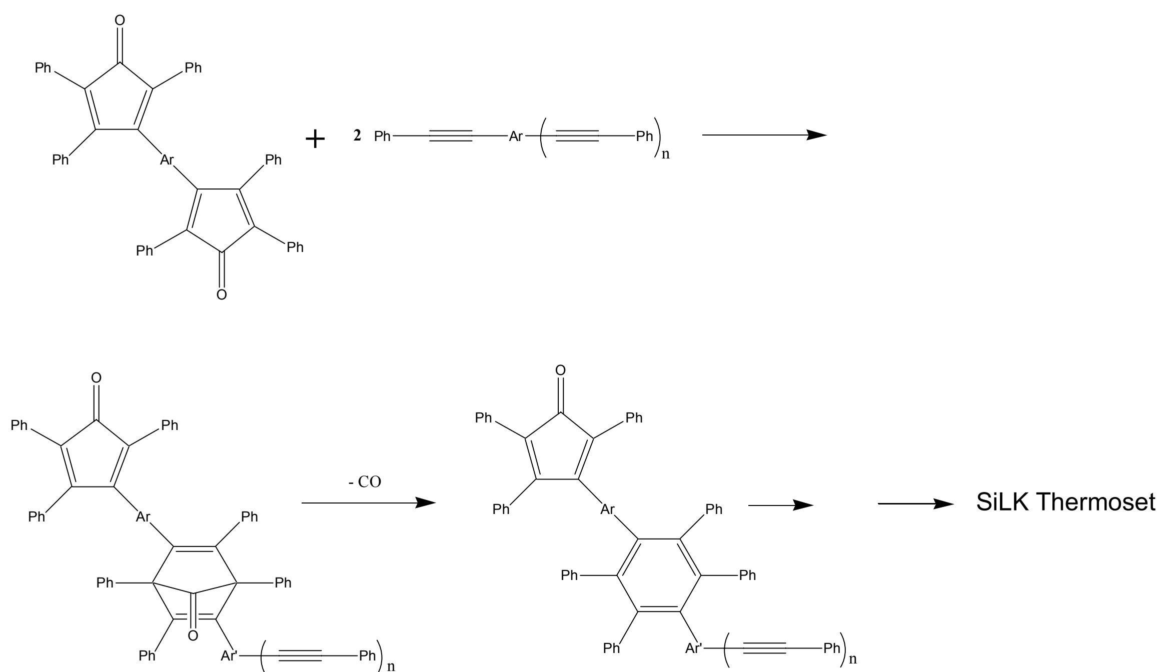

Table 1. Key properties of silicon oxide and SiLK low-*k* material

Properties	SiLK™	Silicon Oxide
Platform	Spin-on organic thermoset	Silicon oxide
Composition (C/O/Si/H)	98 (C+H)/2 O	0/62/32/6/
Dielectric Constant K	2.65	4.3
Breakdown Field (MV/cm^2)	4.5	11
Elastic Modulus (GPa)	3	55 to 70
Hardness (GPa)	0.6	7
Film Stress on Si (MPa)	56	-200
CTE ($ppm/^oC$)	60 to165	0.45
Thermal Conductivity (W/mK)	0.18	1.2

Table 2. Impurity Contents of the As-Received Silica Nanoparticle Solution

Analyte	Amount	Unit
Na_2O	0.51	%
Al_2O_3	770	ppm
TiO_2	64	ppm
ZrO_2	16	ppm
Fe_2O_3	10	ppm
CaO	4	ppm
MgO	4	ppm
Cr	190	ppb
Zn	70	ppb
Pb	40	ppb
Ni	30	ppb
Cu	20	ppb

Figure 1a. TEM micrographs of a SiLK-I nanocomposite thin film with a 19.7 % by volume of silica nanoparticle

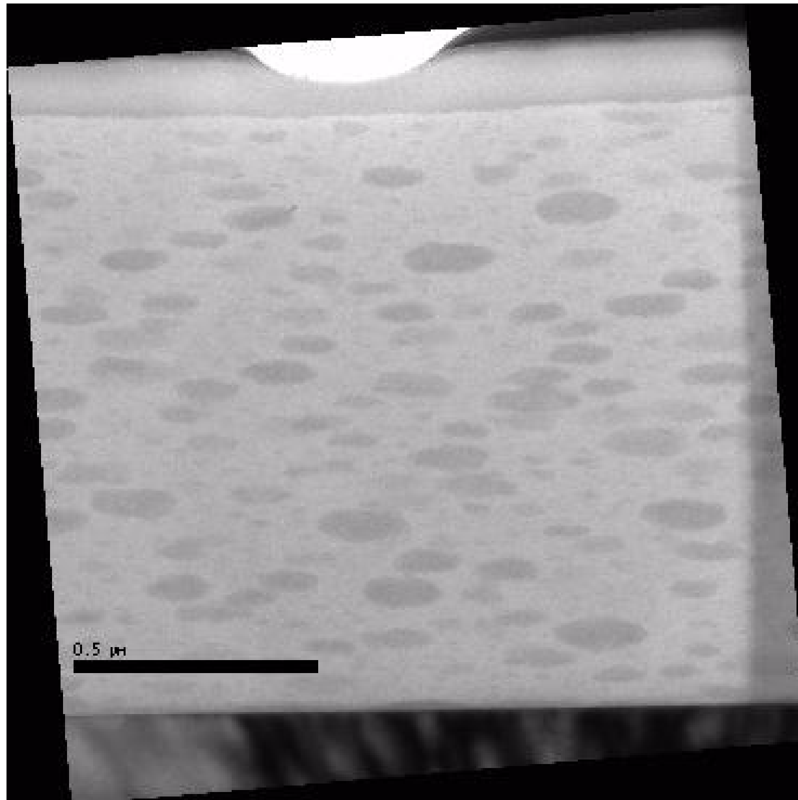

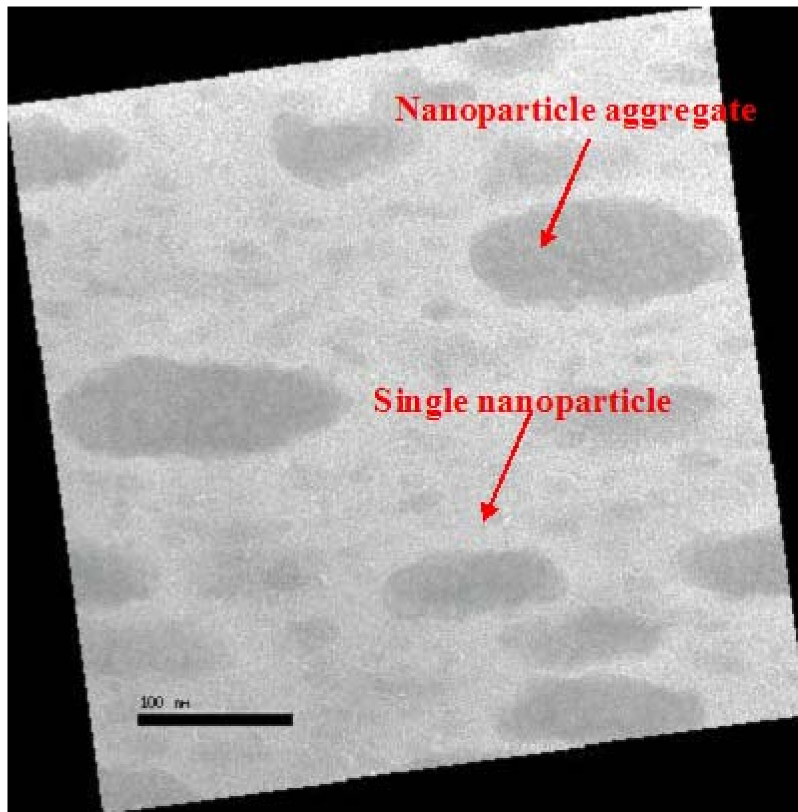

Figure 1b. TEM micrographs of a SiLK-I nanocomposite thin film with a 19.7 % by volume of silica nanoparticle

Figure 2. Effect of silica nanoparticle concentration on the modulus of nanocomposite thin films as measured by nanoindentation and comparison of the measured modulus values of SiLK-I (filled square) and SiLK-D (filled circle) nanocomposite thin films with those predicted by the Halpin-Tsai equations

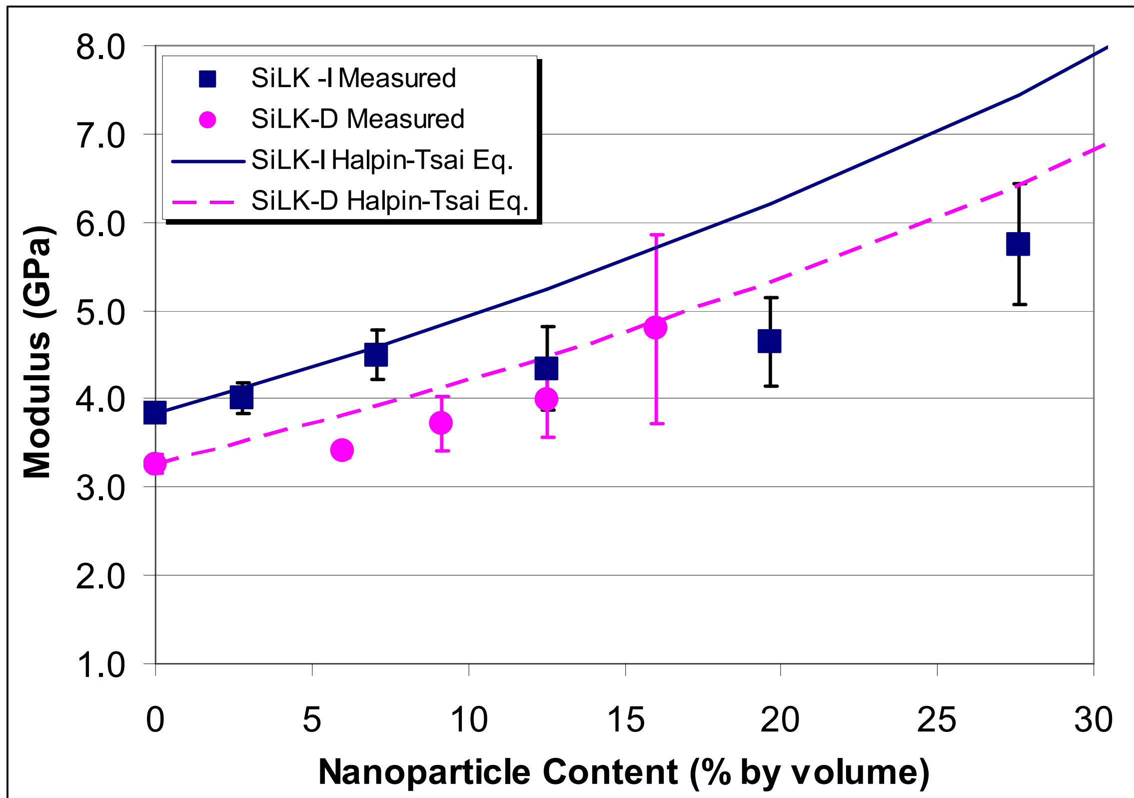

Figure 3. Effect of silica nanoparticle concentration on the hardness of nanocomposite thin films as measured by nanoindentation. Filled square -- SiLK-I; filled circle – SiLK-D

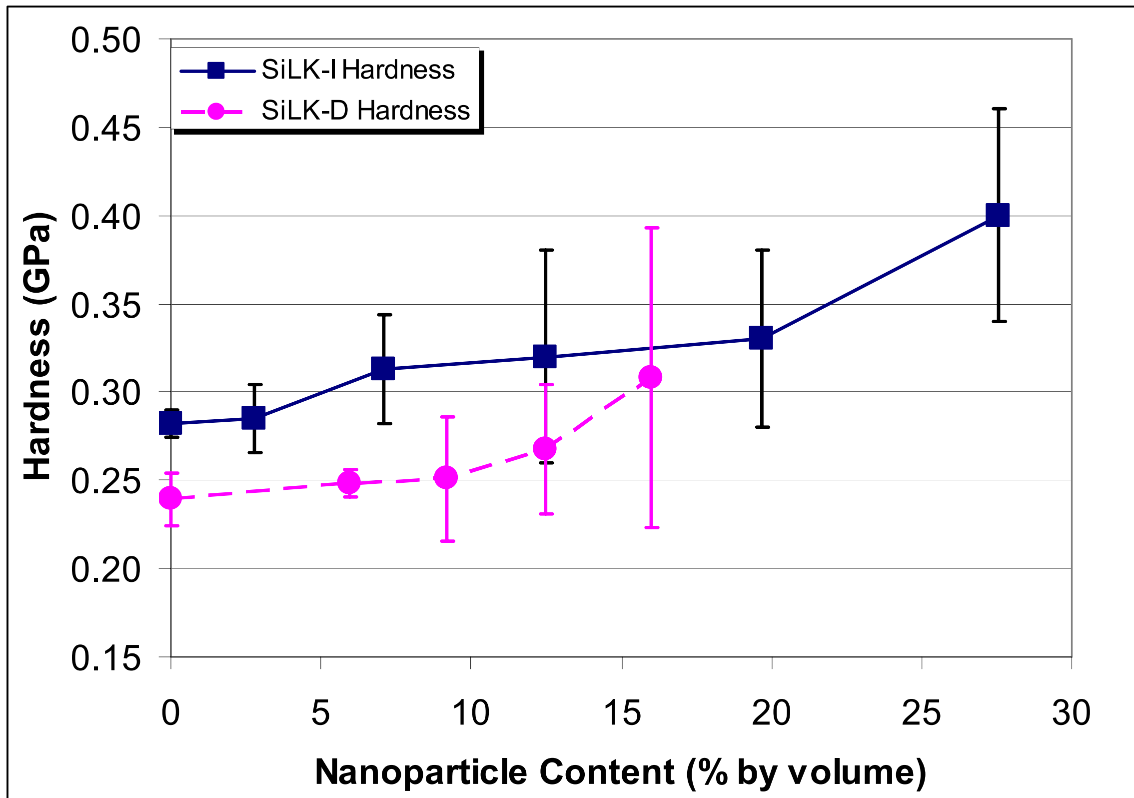

Figure 4. Film thickness at various temperatures as measured by X-ray reflectivity. S-00: neat SiLK-I film. S-007: SiLK-I nanocomposite film with 12.5 % by volume of silica nanoparticle

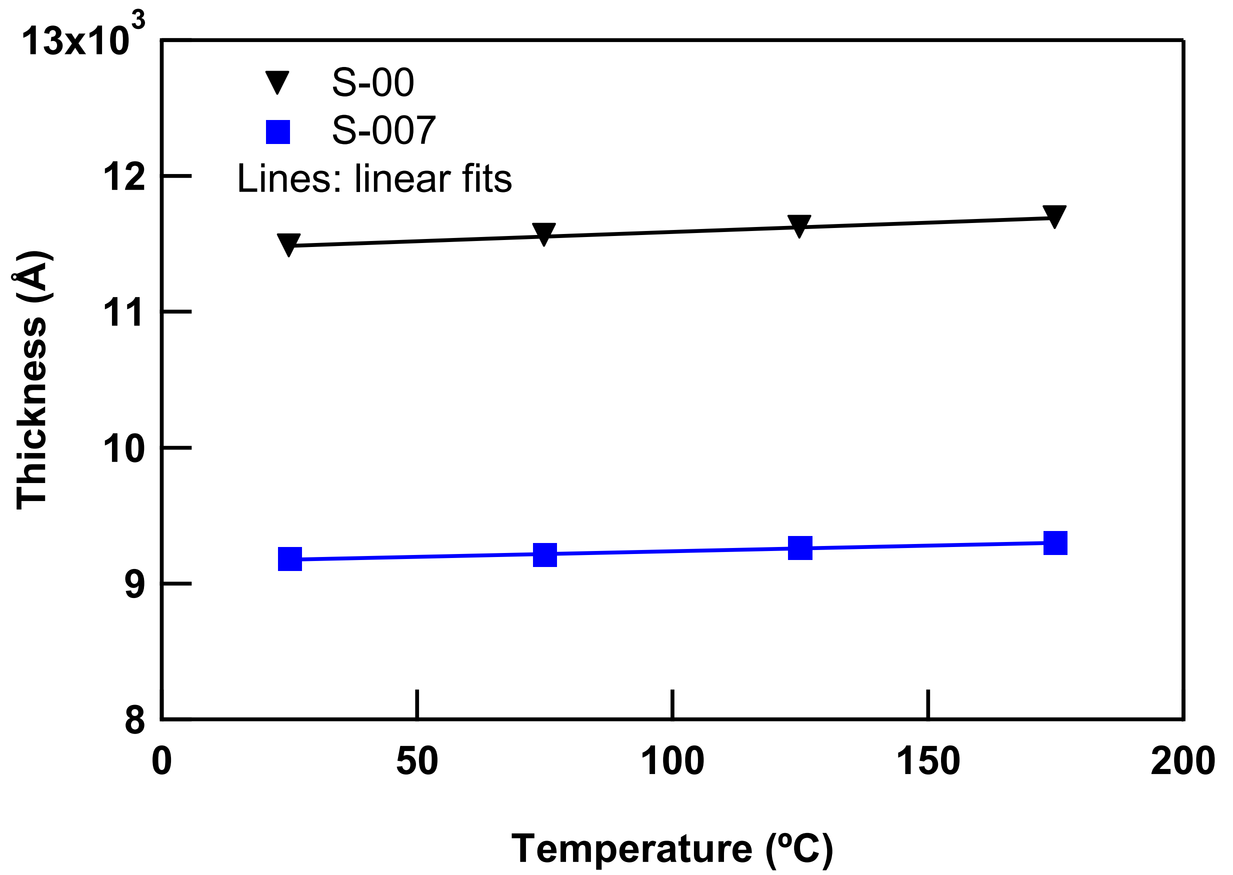

Figure 5. Effect of silica nanoparticle concentration on the relative dielectric constant of SiLK-I (5a) and SiLK-D (5b) nanocomposite thin films and comparison of the measured relative dielectric constant values of SiLK-I (5a) and SiLK-D (5b) nanocomposite thin films with those predicted by the additive formula described in the text.

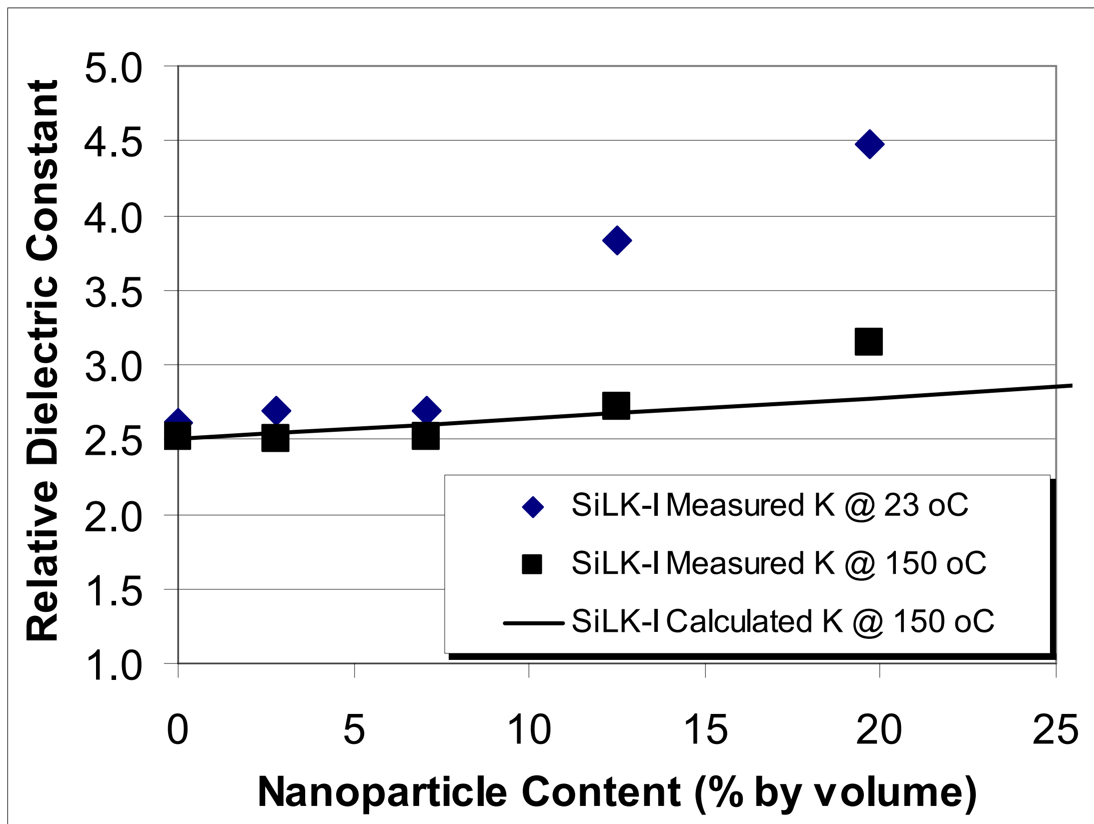

Figure 5. Effect of silica nanoparticle concentration on the relative dielectric constant of SiLK-I (5a) and SiLK-D (5b) nanocomposite thin films and comparison of the measured relative dielectric constant values of SiLK-I (5a) and SiLK-D (5b) nanocomposite thin films with those predicted by the additive formula described in the text.

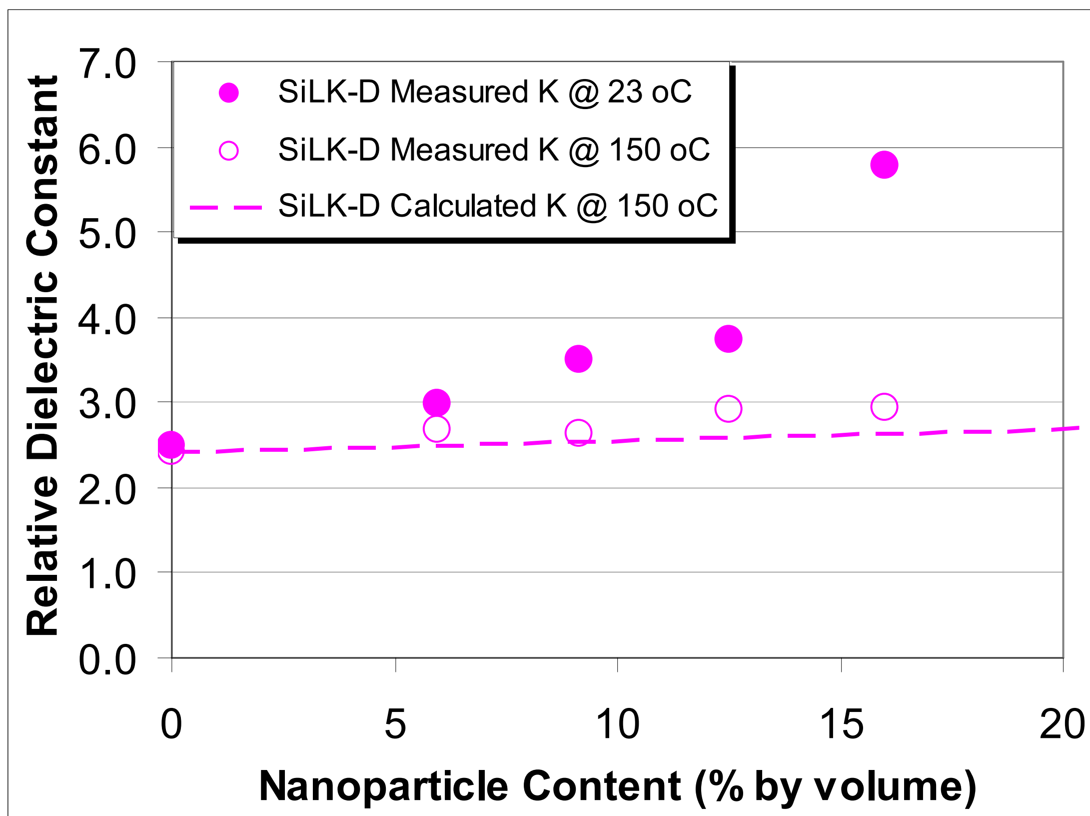

Figure 6. Electrical current density *vs*. field (J-V) curves of SiLK-I nanocomposite thin films with various silica nanoparticle contents.

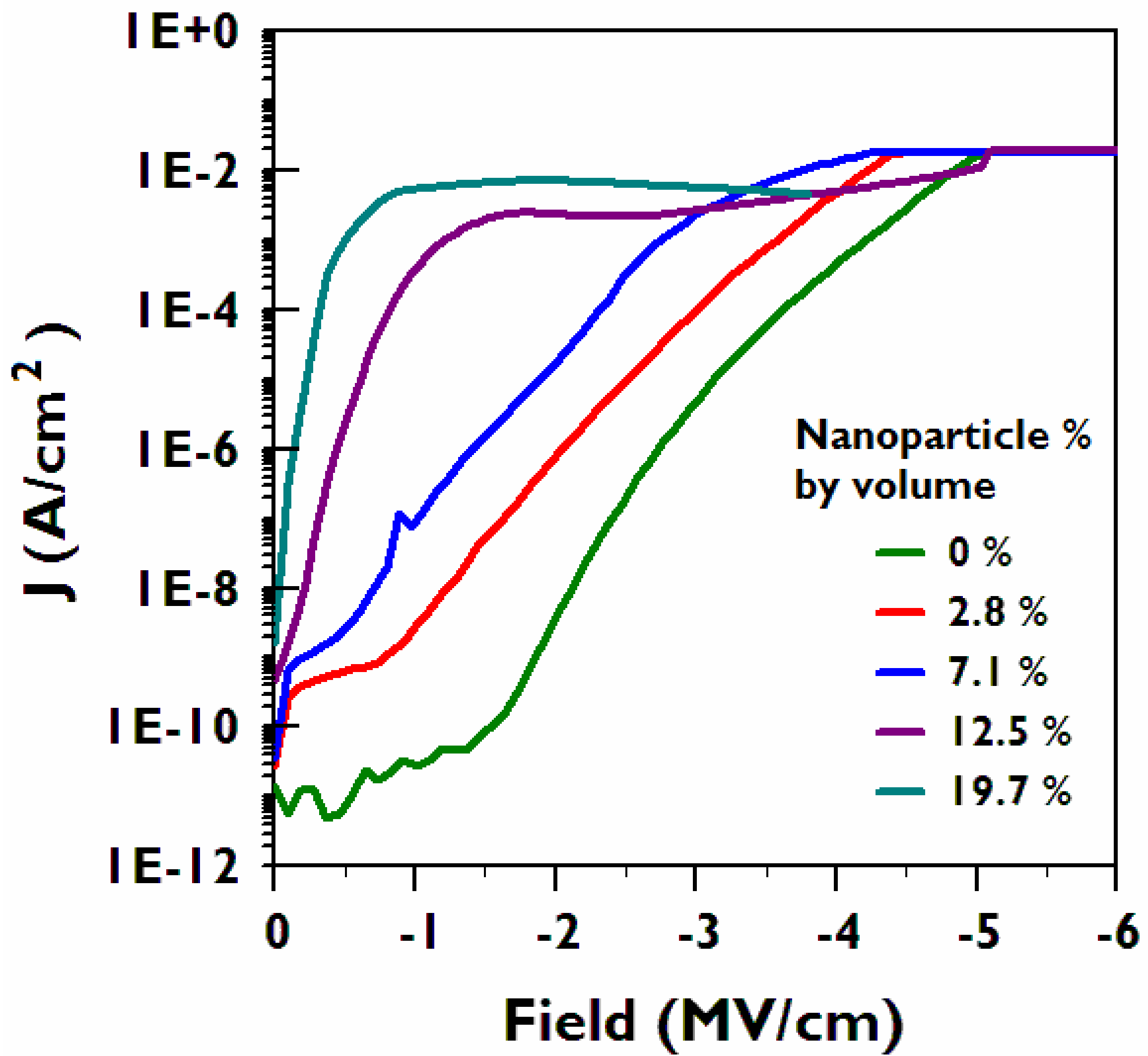

Figure 7. Effect of silica nanoparticle concentration on the dielectric breakdown field of SiLK-I nanocomposite thin films.